

Influence of molecular structure and microstructure on device performance of polycrystalline pentacene thin-film transistors

Horng-Long Cheng,^{a)} Yu-Shen Mai, Wei-Yang Chou, and Li-Ren Chang
*Institute of Electro-Optical Science and Engineering, Center for Micro/Nano Technology Research,
 National Cheng Kung University, Tainan 701, Taiwan*

(Received 18 January 2007; accepted 2 April 2007; published online 27 April 2007)

The authors have fabricated the pentacene thin films on polymethylmethacrylate (PMMA) and on silicon dioxide dielectric surfaces featuring similar surface energy and surface roughness. On both surfaces the pentacene films displayed high crystal quality from x-ray diffraction scans, although the film on PMMA had significantly smaller grain size. The pentacene transistors with PMMA exhibited excellent electrical characteristics, including high mobility of above $1.1 \text{ cm}^2/\text{V s}$, on/off ratio above 10^6 , and sharp subthreshold slope below 1 V/decade . The analysis of molecular microstructure of the pentacene films provided a reasonable explanation for the high performance using resonance micro-Raman spectroscopy. © 2007 American Institute of Physics. [DOI: 10.1063/1.2734370]

The performance of organic thin-film transistors (OTFTs) has greatly improved lately. In particular, we can see performance improvements in conjugated oligoacenes, i.e., pentacene.¹⁻³ Pentacene, deposited on dielectric surfaces with surface-induced structure, forms a polycrystalline thin film with grain morphology.¹ General assumptions suggest that mobility properties appear to be dominated by grain boundary effects that occur due to the large amount of charged trapping states at the boundary.^{1,2,4} Most researchers utilize crystal structure and grain size to interpret the performance of OTFTs. However, some reported data are not consistent with the observations presented above.^{3,5,6} Whether in the intragrain or in grain boundary of organic film, the structures still have weak van der Waals forces, unlike the inorganic polycrystalline media. However, little is known about the importance of molecular structure and microstructure within a polycrystalline organic film on OTFT performance.

Surface properties of a dielectric layer, i.e., surface energy (γ_s) and surface roughness (R_{rms}), are the distinctive factors that determine potential improvements in electric characteristics of OTFT.⁷ Polymeric insulators have been considered as a preferable surface modification layer and/or gate dielectric materials due to their numerous advantages over inorganic materials. Therefore, in addition to studying the γ_s and R_{rms} , it is also interesting to explore the influence of polar groups of polymer insulators on the structure of organic semiconductors and the corresponding performance of OTFTs.

In this letter, we have investigated the crystal structure, thin-film morphology, and molecular structure and microstructure of pentacene films grown on the polymeric and inorganic dielectric surfaces with similar γ_s and R_{rms} values. Hence, the impact of different γ_s and R_{rms} values could be distinguished. The study includes silicon dioxide (SiO_2 , $\gamma_s = 49.8 \text{ mJ/m}^2$, $R_{\text{rms}} = 4.8 \text{ \AA}$) and polymethylmethacrylate (PMMA) ($\gamma_s = 49.1 \text{ mJ/m}^2$, $R_{\text{rms}} = 5.0 \text{ \AA}$) surfaces. We should note that the pentacene film, grown on PMMA surface with a very small grain size, allows the production of OTFTs with very good performance characteristics. Here, we used x-ray diffraction (XRD), atomic force microscope

(AFM), and resonance micro-Raman measurements to discuss possible triggers of enhanced mobility in pentacene-based OTFTs featuring PMMA modifications.

Heavily doped *n*-type Si (111) wafers were used as substrates and gate electrodes. A 3000 \AA SiO_2 layer, thermally grown on the substrate, was used as the gate dielectric. PMMA modified surface upon SiO_2 gate dielectric was fabricated as follows: A 600 \AA PMMA (molecular weight = $540\,000$, obtained from Scientific Polymer Products, Inc.) layer was deposited by spin coating directly onto a SiO_2 layer using a $1 \text{ wt } \%$ PMMA solution from *p*-xylene. The PMMA layer was baked for 4 h at the temperature of $120 \text{ }^\circ\text{C}$. Pentacene films (Acros Organics, purity $\sim 98\%$) were produced by vacuum evaporation onto dielectric surfaces with a thickness of 700 \AA . The deposition rate of approximately 0.5 \AA/s and pressure of $1 \times 10^{-5} \text{ torr}$ were applied and the substrate was maintained at room temperature. The R_{rms} values were measured by AFM (Digital Instrument Multimode SPM AS-12VMF). The γ_s was analyzed from the measured contact angles (FACE contact-angle meter, Kyowa Kaimenkagaku Co.) and the method has been described previously.⁷ The pentacene films were studied by XRD in the symmetric reflection coupled θ - 2θ arrangement. XRD patterns were obtained using $\text{Cu K}\alpha$ radiation ($\lambda_{\text{K}\alpha_1} = 1.5406 \text{ \AA}$) and a wide-angle graphite monochromator. Raman spectra, produced by lattice phonons, were obtained using a Jobin Yvon LabRam HR spectrometer. A 633 nm He-Ne laser served as the excitation light source. The laser's power was kept below 0.5 mW to prevent thermal damage of the pentacene thin film. The spatial resolution of the beam spot was around $1 \text{ }\mu\text{m}$. The resolution measurements were obtained using a $100\times$ objective microscope lens. At least three spectra were measured for each sample and every Raman spectrum was taken an average of 20 times. For deposited pentacene films on the same substrates, the Raman spectra are substantially the same. Electrical characteristics of OTFTs were measured by a Keithley 4200-SCS semiconductor parameter analyzer in a dark vacuum chamber.

Figure 1 shows the XRD spectra of pentacene film grown on PMMA and SiO_2 surfaces. Both films have two major diffraction peaks, which can be attributed to "thin-film phase" ($00l'$) and "triclinic bulk phase" ($00l$), respectively.^{8,9}

^{a)}Electronic mail: shlcheng@mail.ncku.edu.tw

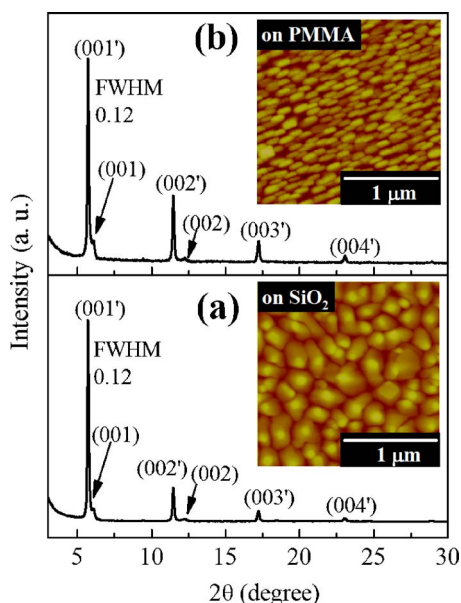


FIG. 1. (Color online) XRD spectra of pentacene films grown on (a) SiO₂ surface and (b) PMMA surface. Inset: The corresponding AFM micrographs.

We observed the same 2θ of (001') peak indicating the thin-film phase with the same interlayer spacing of 15.4 Å, for both pentacene films. The XRD spectra results, combined with paracrystal theory, allow us to estimate the mean dimension of the crystallites (L_{00l}) perpendicular to the plane (00 l) and the distance fluctuation between successive planes of the family (00 l) (g_{11}). Our measurements were based on the full width at half maximum (FWHM) of the diffraction peaks, thus repeating the methodology used in previous reports.^{8,9} The estimated $L_{00l'}$ and g_{11} values of pentacene film grown on PMMA (values for SiO₂ surface are shown in brackets) were equal to 351 ± 9 Å (352 ± 19 Å) and $1.50 \pm 0.06\%$ ($1.48 \pm 0.14\%$), respectively. XRD analysis shows that both pentacene films have a similar crystal quality. However, we can see in the inset of Fig. 1(a) that the pentacene film has significantly smaller grain size on the PMMA surface as compared to the film on the SiO₂ surface. Similar to the previously demonstrated results, the overall nucleation density is higher on the PMMA surface than on the SiO₂ surface at early stages,¹⁰ despite the difference in the experimental conditions. The observed differences between PMMA and SiO₂ substrates were attributed to the difference in the adsorption energy and surface diffusion of pentacene. Here, the R_{rms} and γ_s of the PMMA and SiO₂ surfaces were almost the same. We can therefore conclude that the polar groups on PMMA surface have a great influence on the morphology of pentacene film.

The molecular structure and microstructure of both pentacene films on PMMA and on SiO₂ surface were studied using resonance micro-Raman spectroscopy. We used red excitation line ($\lambda_{\text{exc}} = 633$ nm) with the wavelength that was located precisely at the absorption peak arising from the intermolecular interactions, so-called the Davydov splitting.^{11,12} We expected to see a resonance enhancement of these modes related to Davydov splitting in Raman spectra. As shown in Fig. 2, we focused on the C–H in-plane bending (1140–1190 cm⁻¹ region) and the C–C aromatic stretching (1340–1390 cm⁻¹ region) vibrations. These modes have been assumed to contribute to the relaxation (reorganization) en-

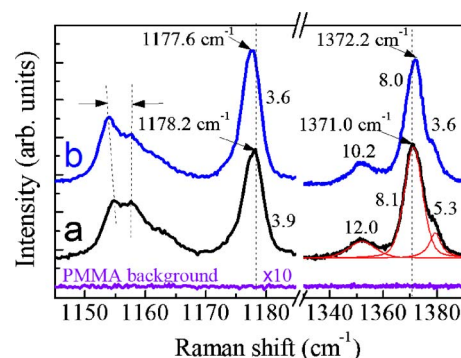


FIG. 2. (Color online) Raman spectra of pentacene films grown on SiO₂ (trace a) and PMMA (trace b). The dashed lines serve as guidelines. The FWHMs of selected Raman bands are also shown. The spectrometer resolution is 0.2 cm⁻¹.

ergy most intensively;¹³ therefore one can expect to see the impact of the modes on the conformational transition during the carrier transport process. Moreover, there is no detectable Raman band of PMMA film on the SiO₂ surface in the energy range of 1100–1400 cm⁻¹. The 1158 (A_g) and 1178 cm⁻¹ (A_g) modes that originate from a pentacene molecule are assigned to the motion of atoms located at the end and on both sides of the pentacene molecule, respectively.^{11,14} For the C–C aromatic stretching mode, there were three bands found at 1351 (A_g), 1370 (A_g), and 1379 (B_{3g}) cm⁻¹.¹⁴ First, we have noticed that the FWHM of the 1178 cm⁻¹ band and C–C aromatic stretching modes were smaller on the PMMA surface as compared to the SiO₂ surface. The smaller FWHM implied that pentacene molecule in the thin film on PMMA was more homogeneous, thus the lower molecular relaxation energy. Second, we observed opposite shifts of the frequency for the strongest C–H in-plane bending mode and the strongest C–C stretching mode. The opposite shift trends in Raman spectra have also been observed in other π -conjugated molecular materials during measured temperature decreases,¹⁵ indicating that the unit cell volume was reduced. Third, a splitting ($\Delta\nu$) between 1158 and 1155 cm⁻¹ was larger on the PMMA surface than on the SiO₂ based surface. Previously, the bands at around 1155 cm⁻¹ have been explained by Davydov splitting supported by the fact that the intensity ratio depends on the polarization.¹¹ The relative intensity I_{1155}/I_{1158} was equal to 1.25 ± 0.10 and 1.85 ± 0.21 for pentacene films grown on SiO₂ and PMMA surfaces, respectively. Indeed, we have found that the 1155 cm⁻¹ band is related to the intermolecular coupling in the direction parallel to the a - b lattice plane¹⁴ and highly sensitive in response to 633 nm excitation lines as compared to other Raman modes. The obtained results indicate that there were stronger interactions between the adjacent pentacene molecules of the film based on the PMMA surface. Additionally, we have made complementary low temperature Raman measurements for experimental pentacene films (data not shown). The significant upward shift of the 1370 cm⁻¹ band is associated with an increase in $\Delta\nu$ and can be viewed as evidence supporting increased intermolecular interactions. Along with the decrease in temperature, we could observe enlarged Davydov splitting in optical absorption spectra of pentacene thin-film phase. Enlarged Davydov splitting has also been predicted by Faltermeier *et al.* recently.¹²

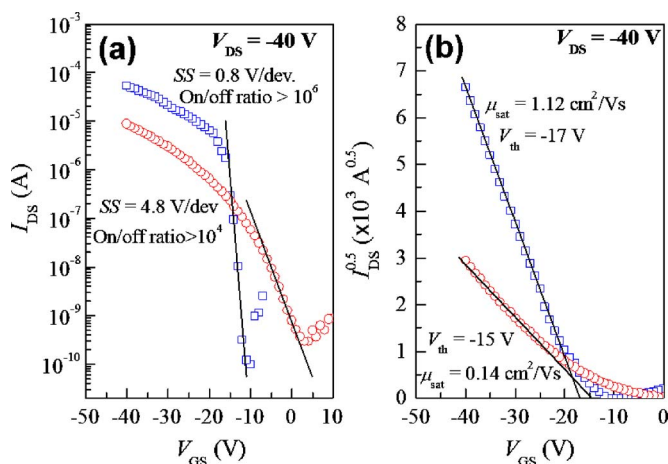


FIG. 3. (Color online) Transfer electrical characteristics of silver top-contact pentacene OTFTs with (\square) and without (\circ) PMMA modification layer (channel length=120 μm , channel width=1920 μm).

Next, we turn our attention to the performance of the OTFT devices produced using pentacene films deposited on PMMA and SiO_2 surfaces, respectively. Figure 3 shows the typical transfer characteristics of OTFT devices. The devices, with pentacene film deposited onto PMMA surface, exhibit better performance than the devices featuring pentacene films deposited onto the SiO_2 surface. The devices featuring PMMA layer had the modulated on/off current ratio larger than 10^6 , while the subthreshold slope (SS) was equal to 0.7–1.0 V/decade. Low value of SS indicated a very low density of deep traps at the interface and the formation of the ideal field-effect channel in pentacene OTFTs with PMMA layer. The saturated field-effect mobility (μ_{sat}) reached above $1.1 \text{ cm}^2/\text{V s}$ (with average values falling in the range of 0.8–1.2 $\text{cm}^2/\text{V s}$). On the opposite, the devices without PMMA displayed poor performance, μ_{sat} with values found within the range of 0.06–0.3 $\text{cm}^2/\text{V s}$. Additionally, we have also fabricated gold top-contact OTFTs, for which we observed similar μ_{sat} indicating that the contact resistance has a minor effect on pentacene film growth on PMMA when operating at the saturation regime. Moreover, pentacene-based OTFTs may exhibit hysteresis that alters the slope of transfer characteristics.¹⁶ Here, we have not observed the significant influence of the hysteresis effects on the measured mobilities for both devices. Similarly, Uemura *et al.*¹⁷ have not observed the hysteresis effect of pentacene-based OTFTs using PMMA as gate dielectric due to the PMMA having disordered dipole moment. De Angelis *et al.* have shown that PMMA is a good buffer layer between pentacene and SiO_2 .¹⁸ Thus, the improved device performance was attributed to better molecular microstructure of pentacene film on PMMA surface, including larger intermolecular interactions and lower molecular relaxation energy due to great environmental homogeneity. Obviously, the increased density of grain boundaries does not show a negative effect on device performance.

In conclusion, this study gives clear experimental evidence that the pentacene grown on the PMMA surface had better molecular microstructure as compared to the film

based on the SiO_2 surface. However, the results of XRD scans show that the crystal structure and crystal quality of both pentacene films are virtually the same. At the same time, the film on the PMMA surface has significantly smaller grain size. Therefore, we argued that the well-ordered crystalline structure and/or large grain size are not enough to reflect the optimized supramolecular structure of polycrystalline organic film for efficient charge transportation. Our observations are different from previous expectations¹⁹ where higher nucleation density of pentacene on PMMA surface should influence the amount of grain boundaries, which may act as charge carrier traps and consequently degrade OTFT characteristics. On the contrary, we have fabricated high performance pentacene-based OFET with a PMMA modification layer. Consequently, we believe that the study of molecular microstructure of polycrystalline organic films is an area of immense importance and interest.

The authors acknowledge financial support from National Science Council, Taiwan, through Grant No. NSC 95-2221-E-006-430. The authors also acknowledge the National Center for High-performance Computing, Taiwan.

¹C. D. Dimitrakopoulos and P. R. L. Malenfant, *Adv. Mater.* (Weinheim, Ger.) **14**, 99 (2002), and references therein.

²Y.-Y. Lin, D. J. Gundlach, S. F. Nelson, and T. N. Jackson, *IEEE Trans. Electron Devices* **44**, 1325 (1997).

³T. W. Kelley, D. V. Muires, P. F. Baude, T. P. Smith, and T. D. Jones, *Mater. Res. Soc. Symp. Proc.* **771**, 169 (2003); S. Lee, B. Koo, J. Shin, E. Lee, H. Park, and H. Kima, *Appl. Phys. Lett.* **88**, 162109 (2006).

⁴G. Horowitz, *Adv. Funct. Mater.* **13**, 53 (2003), and references therein.

⁵D. Knipp, R. A. Street, A. Völkel, and J. Ho, *J. Appl. Phys.* **93**, 347 (2003).

⁶M. Shtein, J. Mapel, J. B. Benziger, and S. R. Forrest, *Appl. Phys. Lett.* **81**, 268 (2002).

⁷W. Y. Chou, C. W. Kuo, H. L. Cheng, Y. R. Chen, F. C. Tang, F. Y. Yang, D. Y. Shu, and C. C. Liao, *Appl. Phys. Lett.* **89**, 112126 (2006), and references therein.

⁸T. Minakata, H. Imai, M. Ozaki, and K. Saco, *J. Appl. Phys.* **72**, 5220 (1992).

⁹C. D. Dimitrakopoulos, A. R. Brown, and A. Pomp, *J. Appl. Phys.* **80**, 2501 (1992).

¹⁰B. Stadlober, U. Haas, H. Maresch, and A. Haase, *Phys. Rev. B* **74**, 165302 (2006).

¹¹T. Jentzsch, H. J. Juepner, K. W. Brzezinka, and A. Lau, *Thin Solid Films* **315**, 273 (1998).

¹²D. Faltermeier, B. Gompf, M. Dressel, A. K. Tripathi, and J. Pflaum, *Phys. Rev. B* **74**, 125416 (2006).

¹³O. Kwon, V. Coropceanu, N. E. Gruhn, J. C. Durivage, J. G. Laquindanum, H. E. Katz, J. Cornil, and J.-L. Brédas, *J. Chem. Phys.* **120**, 8186 (2004).

¹⁴H. L. Cheng, W. Y. Chou, C. W. Kuo, F. C. Tang, and Y. W. Wang, *Appl. Phys. Lett.* **88**, 161918 (2006); H. L. Cheng, W. Y. Chou, C. W. Kuo, Y. S. Mai, F. C. Tang, and S. H. Lai, *Proc. SPIE* **6336**, 63361B (2006).

¹⁵B. Toudic, P. Limelette, G. Froyer, F. Le Gac, A. Moréac, and P. Rabiller, *Phys. Rev. Lett.* **95**, 215502 (2005).

¹⁶G. Gu, M. G. Kane, J. E. Doty, and A. H. Firester, *Appl. Phys. Lett.* **87**, 243512 (2005).

¹⁷S. Uemura, A. Komukai, R. Sakaida, T. Kawai, M. Yoshida, S. Hoshino, T. Kodzasa, and T. Kamata, *Synth. Met.* **153**, 405 (2005).

¹⁸F. De Angelis, S. Cipolloni, L. Mariucci, and G. Fortunato, *Appl. Phys. Lett.* **86**, 203505 (2005).

¹⁹S. Pratontep, F. Nüesch, L. Zuppiroli, and M. Brinkmann, *Phys. Rev. B* **72**, 085211 (2005).